

## Isolation and identification of *Streptomyces murinus* XF-3 and its active metabolite actinomycin D against root rot disease of American ginseng

Qiu YuHao<sup>1</sup>, Liang WenJing<sup>1</sup>, Li MeiQi<sup>1</sup>, Zhu Hong<sup>1</sup>, Peng Hao<sup>1\*</sup>, Si DouDou<sup>1</sup>, Xie YuSi<sup>2</sup>

<sup>1</sup>Shaanxi University of Technology, Hanzhong 723001, Shaanxi, China

<sup>2</sup>Shaanxi Agricultural Radio and Television School, Hanzhong 724400, Shaanxi, China

\*Corresponding author's email: huaohao808@126.com

Received: 09 September 2025 / Revised: 14 January 2026 / Accepted: 24 January 2026 / Published Online: 16 February 2026

### Abstract

To address the severe threat of root rot caused by *F. solani* and *F. oxysporum* to American ginseng production and the limitations of chemical control, this study aimed to screen antagonistic actinomycetes and identify their key active substances. Actinomycetes were isolated from the rhizosphere soil of healthy American ginseng using the dilution plate method, and antagonistic strains were screened via the mycelial growth rate assay. Strain XF-3, with the highest inhibitory activity, was identified as *S. murinus* based on morphological, physiological-biochemical, and 16S rDNA sequence analyses. Its fermentation broth exhibited in vitro control efficacies of 56.09% and 66.27% against *F. solani* and *F. oxysporum*, respectively, in detached root inoculation tests. The key active metabolite was isolated via column chromatography and identified as actinomycin D using NMR and LC-MS. Mycelial growth inhibition assays showed EC<sub>50</sub> values of actinomycin D against *F. solani* and *F. oxysporum* were 2.08 µg/mL and 11.48 µg/mL, respectively. This study provides a candidate biocontrol strain *S. murinus* XF-3 and theoretical basis for the green management of American ginseng root rot, while expanding the application scope of actinomycin D in agricultural biocontrol.

**Keywords:** American ginseng root rot, *Fusarium oxysporum*, *Fusarium solani*, Metabolites, Actinomycin D

### How to cite this article:

YuHao Q, WenJing L, MeiQi L, Hong Z, Hao P, DouDou S and YuSi X. Isolation and identification of *Streptomyces murinus* XF-3 and its active metabolite actinomycin D against root rot disease of American ginseng. Asian J Agric. Biol. 2026: e2025270. DOI: https://doi.org/10.35495/ajab.2025.270

This is an Open Access article distributed under the terms of the Creative Commons Attribution 4.0 License. (https://creativecommons.org/licenses/by/4.0), which permits unrestricted use, distribution, and reproduction in any medium, provided the original work is properly cited.

## Introduction

American ginseng (*Panax quinquefolius L.*) is a perennial herbaceous plant belonging to the Araliaceae family. Its roots possess significant medicinal properties, including the ability to tonify qi, nourish yin, and promote fluid production, making it one of China's important economic crops (National Pharmacopoeia Committee, 2022). Since its successful introduction in the 1980s, China has become the world's second-largest producer of American ginseng (Guo et al., 2022). However, the frequent occurrence of root rot disease has severely constrained the sustainable development of the American ginseng industry. This disease is primarily caused by pathogenic fungi of the genus *Fusarium* and affects ginseng roots aged 1-4 years, leading to root tissue decay and even complete crop failure, with disease incidence rates ranging from 10% to 80% (Ji, 2023; Huang, 2021; He and Jia, 2009). Currently, conventional agricultural control methods show limited effectiveness, while chemical control, though providing rapid short-term results, can lead to environmental contamination and pesticide residue accumulation, posing risks to human health, environmental safety, and leading to pesticide residue accumulation in the produce (Zhao, 2020; Zhang et al., 2024). Therefore, developing green and efficient biological control technologies is crucial for addressing root rot disease problems.

Biological control using antagonistic microorganisms and their secondary metabolites has emerged as a promising alternative, offering ecological sustainability and reduced environmental risks (Yu et al., 2011). Among antagonistic microorganisms, *Streptomyces* species are particularly attractive due to their ability to produce diverse antibiotics and promote plant growth via nitrogen fixation and phosphate solubilization (Huang et al., 1998; Wang et al., 2024). Previous studies have reported *Streptomyces* strains with inhibitory activity against ginseng root rot pathogens (Yan et al., 2010; Zhang et al., 2024), but these studies have critical limitations. Most focus only on strain screening without systematic characterization of antimicrobial metabolites, and the control efficacy in practical applications is often unsatisfactory (Zhang et al., 2024). Notably, rhizosphere microorganisms of medicinal plants interact with root exudates over a long period, occupying a crucial ecological niche for the screening of active bacterial strains. Therefore, screening

antagonistic bacteria from the rhizosphere soil of healthy American ginseng is a direct strategy to discover strains that are highly adaptable to the host and can effectively inhibit in-situ pathogenic bacteria (Zhang, 2014). However, current research on biocontrol actinomycetes against ginseng root rot is limited, and existing studies have not elucidated the mechanism by which *Streptomyces* antagonizes *Fusarium* at the metabolite level. This knowledge gap hinders the development of targeted biocontrol agents guided by specific active metabolites.

This study targeted the major pathogens of American ginseng root rot, *F. solani* and *F. oxysporum*, and aimed to isolate and screen antagonistic actinomycetes from healthy American ginseng rhizosphere soil to obtain highly effective biocontrol strains. The research employed morphological, physiological, biochemical, and molecular biological methods for species identification and analysis of antimicrobial active compounds. The results provide new approaches and theoretical foundations for green control of American ginseng root rot, contributing significantly to the development of ecological agriculture and improvement of medicinal material quality.

## Material and Methods

### Soil sample

The soil sample was collected in December 2023 from an American ginseng cultivation area in Liuba County, Hanzhong City, Shaanxi Province. The physicochemical properties of the soil were determined as follows: total nitrogen (TN) 2.00±0.03 g/kg, organic matter (OM) 32.59±0.08 g/kg, total phosphorus (TP) 1.06±0.01 g/kg, total potassium (TK) 24.02±0.37 g/kg, and pH 5.57±0.01.

### Tested strains

*F. solani* and *F. oxysporum* were provided by the Microbial Technology Laboratory of the School of Biological Science and Engineering, Shaanxi University of Technology.

### Culture media

The isolation and purification of actinomycetes were conducted using GS-1 medium; various media such as ISP3-6, PDA, NA, CA, and GS-1 were used for morphological observation and cultivation of the strains; the activation and cultivation of pathogenic bacteria were all carried out on PDA medium; and the

fermentation cultivation of target strains was performed using GS-1 liquid medium (Liu et al., 2025).

### Reagents and instruments

Actinomycin D standard (MCE); Methanol, ethyl acetate, petroleum ether, n-butanol, acetone, chloroform (Tianjin Fuyu Fine Chemical Co., Ltd.); LS-150LD vertical pressure steam sterilizer (Jiangyin Binjiang Medical Equipment Co., Ltd.); RV8 rotary evaporator (IKA); BSP-400 biochemical incubator (Shanghai Boxun Industrial Co., Ltd. Medical Equipment Plant); 5977B Agilent GC-MS system; C18 chromatographic column (250 × 4.6 mm, 5 μm, Dikma Technologies).

### Isolation and purification of actinobacteria

Actinobacteria were isolated from the soil of healthy American ginseng using the dilution plate coating method. A 25 g soil sample was mixed with 225 mL of sterile water and shaken at 28°C and 180 rpm for 30 minutes. Subsequently, the mixture was diluted to concentrations of 10<sup>-2</sup> to 10<sup>-6</sup> under aseptic conditions. Aliquots (100 μL) from the 10<sup>-4</sup>, 10<sup>-5</sup>, and 10<sup>-6</sup> dilutions were spread onto isolation medium plates supplemented with 50 μg/mL cycloheximide and 50 μg/mL potassium dichromate. The sealed plates were incubated upside down at 28°C for 5-30 days, ensure the maximum isolation of actinomycete resources with rich diversity and potential biological activity (Zheng et al., 2006). Colonies exhibiting distinct morphologies were selected daily and transferred to fresh GS-1 solid medium for purification and storage.

### Screening of antagonistic actinomycetes

The mycelial growth rate method (Li, 2017) was employed to determine the effect of antagonistic bacterial fermentation broth on pathogenic fungal mycelial growth. A small amount of actinomycete spores was inoculated into conical flasks containing 100 mL of Gause's medium No.1 and cultured on a shaker at 200 r·min<sup>-1</sup> for 7 days. The fermentation broth was centrifuged to obtain the supernatant, which was then filtered through a 0.22 μm membrane filter and mixed with molten PDA medium at a ratio of 1:9 (v:v) to prepare the fermentation broth medium. The control group (CK) consisted of PDA medium with an equal volume of sterile water added. Fungal discs of the test pathogenic fungi were obtained using a 6 mm cork borer and inoculated at the center of both the

fermentation broth medium and PDA medium plates. After incubation at 25°C for 3 days, the diameters of the treated fungi were recorded using the cross-measurement method, and inhibition rates were calculated.

Inhibition rate (%) = [(Control colony diameter - disc diameter) - (Treatment colony diameter - disc diameter)] / (Control colony diameter - disc diameter) × 100%.

### Identification of antagonistic bacterial strains

#### Morphological identification

The spores of the tested strains were streaked onto five types of media: ISP3, ISP4, ISP6, CA, and GS-1. After incubation at 28°C for 14 days, the growth status, colony color, and pigment production of the strains were observed and recorded (Li et al., 2025).

#### Physiological and biochemical characterization

A series of physiological and biochemical tests were performed following the methodology described by Guo et al. (Guo et al., 2024). These tests included starch hydrolysis, gelatin liquefaction, milk peptonization, hydrogen sulfide production, lipase activity, casein hydrolysis, catalase activity, urease activity, cellulose hydrolysis, nitrate reduction, and utilization of various carbon and nitrogen sources. The results were used to make a preliminary inference regarding the taxonomic classification of the strain.

#### Molecular biological identification

Genomic DNA of the target strains was extracted using a bacterial genomic DNA extraction kit (Sangon Biotech, Shanghai). The 16S rDNA was amplified using universal bacterial primers 27F (5'-AGAGTTTGATCMTGGCTCAG-3') and 1492R (5'-ACGGTTACCTTACCTTGTTACGACTT-3'). The amplified PCR products were sent to Sangon Biotech for sequencing. The assembled sequences were uploaded to the NCBI website for BLAST comparison, and related sequences were downloaded. Using *Nocardia aobensis* as the outgroup, a phylogenetic tree was constructed by the Neighbor-Joining method for cluster analysis to identify the target strains.

### Fermentation broth efficacy testing

Healthy American ginseng roots were surface sterilized, and 20  $\mu\text{L}$  of crude fermentation broth and pathogenic fungal spore suspension at a concentration of  $1 \times 10^7$  spores/mL were injected beneath the root epidermis using sterile syringes. Sterile water served as the control (CK), resulting in six treatments: 20  $\mu\text{L}$  sterile water (CK group), 20  $\mu\text{L}$  sterile fermentation broth (group 1), 20  $\mu\text{L}$  *F. oxysporum* suspension (group 2), 20  $\mu\text{L}$  *F. solani* suspension (group 3), 20  $\mu\text{L}$  equal mixture of fermentation broth and *F. oxysporum* (group 4), and 20  $\mu\text{L}$  equal mixture of fermentation broth and *F. solani* (group 5). After incubation in darkness at 25°C for 5 days, disease severity grades of American ginseng were determined based on cross-sectional examination: Grade 0: intact cross-section with no disease spots; Grade 1: diseased area less than 1/10 of cross-section; Grade 2: diseased area 1/10-1/3 of cross-section; Grade 3: diseased area 1/3-2/3 of cross-section; Grade 4: diseased area greater than 2/3 of cross-section (Jiao et al., 2019). The root disease index was calculated using the following formula (Sun et al., 2022):

$$\text{Disease index} = \frac{\sum [(\text{Disease grade index} \times \text{Relative grade index}) / (\text{Total number investigated} \times \text{Highest disease grade})] \times 100\%}{}$$

$$\text{Relative control efficacy (\%)} = \frac{(\text{Control disease index} - \text{Treatment disease index}) / \text{Control disease index} \times 100\%}{}$$

### Selection of extraction solvent

Prepare the fermentation broth of strain XF-3 according to the conditions in Method 1.2.2, centrifuge at 5000 rpm for 20 minutes to collect the supernatant, and then take 300 mL of the supernatant separately. Extract with four organic solvents of different polarities: petroleum ether ( $\log P=3.8$ ), n-butanol ( $\log P=0.88$ ), ethyl acetate ( $\log P=0.73$ ), and acetone ( $\log P=-0.24$ ) in equal volumes (1:1, v/v) to efficiently extract metabolites spanning a wide range of polarities (Cao et al., 2011). The extraction is performed under shaking conditions at  $25 \pm 1^\circ\text{C}$  and 120 rpm for 12 hours, repeated three times; the extracts from the same solvent are combined, and then concentrated to dryness under reduced pressure at 40°C and 0.08 MPa. The residue is dissolved in methanol and diluted to 5 mL, filtered through a 0.22  $\mu\text{m}$  organic phase filter membrane, and stored for later use. The antimicrobial activity of active compounds in

different ester phase extracts against *F. solani* and *F. oxysporum* was determined using the agar well diffusion method. Twenty microliters of concentrated extract were added to central wells in PDA plates that had been spread with spore suspensions of *F. solani* and *F. oxysporum* at a concentration of  $1 \times 10^6$  spores/mL. After allowing the liquid in the wells to diffuse, the plates were incubated in a culture chamber. An equivalent volume of methanol served as the blank control. Following incubation in darkness at 25°C for 3 days, the diameter of inhibition zones was measured using the cross-diagonal method. The diameter of inhibition zones was used as the evaluation criterion to compare the antimicrobial efficacy of active compounds in different ester phase extracts and to select the optimal extraction solvent.

### Isolation and purification of active compounds

Ten liters of strain fermentation broth were prepared and centrifuged at 5000 rpm for 20 min to separate the bacterial cells. The supernatant was extracted with the optimal extraction solvent selected in section 1.2.5 until the solution became colorless. The extracts were combined and concentrated under reduced pressure at 40°C to obtain 16.37 g of reddish, fishy-smelling paste-like crude extract. Using the antifungal activity against *F. solani* and *F. oxysporum* as a bioassay-guided fractionation strategy, the crude extract was dissolved in a small amount of ethyl acetate and subjected to normal-phase silica gel column chromatography (200-300 mesh). Gradient elution was performed with petroleum ether-ethyl acetate (volume ratios from 95:5 to 1:4), and eluents were combined based on thin-layer chromatography visualization to obtain five fractions (Fr.1-Fr.5). Through plate confrontation assays, Fr.2 was identified as the major antimicrobial component. Fr.2 was further separated using preparative thin-layer chromatography with ethyl acetate-acetone (volume ratio 8:2) as the developing solvent, yielding two components: Fr.A and Fr.B. Plate confrontation culture assays confirmed that Fr.B possessed antimicrobial activity. After purity testing, Fr.B was dissolved in chloroform, transfer to a nuclear magnetic resonance (NMR) tube for NMR analysis, including  $^1\text{H-NMR}$  and  $^{13}\text{C-NMR}$  spectral analysis, and perform LC-MS/MS determination on the compound.

### Standard curve preparation and quantification of actinomycin D

The actinomycin D content in the fermentation broth was determined using high-performance liquid chromatography (HPLC). A 300 mL sample of the strain's fermentation broth was prepared. Following the extraction and rotary evaporation procedures described in section 1.2.6, the resulting residue was washed with methanol and the volume adjusted to 5 mL. This solution was filtered through a 0.22 µm membrane prior to HPLC analysis for actinomycin D content.

Standard curve preparation: A 5 mg aliquot of actinomycin D standard (commercially purchased, 98% purity) was dissolved in a 60% methanol aqueous solution to prepare standard solutions with concentrations of 1, 2.5, 10, 25, and 50 µg/mL. Referring to the chromatographic conditions specified in Part II of the *Chinese Pharmacopoeia* (National Pharmacopoeia Committee, 2022, volume 2), the HPLC parameters were set as follows: flow rate 1 mL/min, injection volume 20 µL, column temperature 30°C, detection wavelength 443 nm, and a gradient elution from 0 to 100% methanol. The presence of actinomycin D in the sample was confirmed by comparing its retention time and characteristic UV absorption peak with those of the standard. The standard curve was constructed by plotting the peak area (y) against the concentration (x, µg/mL).

### Determination of actinomycin D effects on mycelial growth of *F. solani* and *F. oxysporum* causing American ginseng root rot

Actinomycin D (commercially purchased, 98% purity) was added to PDA medium cooled to 50°C at different ratios to achieve final concentrations of 3, 6, 12, 24, 48, and 96 µg/mL. Pathogenic fungal plugs with a diameter of 6 mm were placed inverted at the center of drug-containing plates and incubated at 25°C for 3 days. Pathogenic fungal plates without actinomycin D served as controls. Colony diameters were measured using the cross-diagonal method, with three replicates for each concentration. The mycelial growth inhibition rates of different actinomycin D concentrations against *F. solani* and *F. oxysporum* were calculated.

Mycelial growth inhibition rate (%) = [(Control group colony diameter - fungal plug diameter) - (Treatment group colony diameter - fungal plug diameter)] / (Control group colony diameter - fungal plug diameter) × 100%. The 'concentration-mycelial growth inhibition rate' data were fitted using a four-parameter logistic model for nonlinear regression to calculate EC<sub>50</sub>. The model formula is as follows:  $Y = \text{Bottom} + (\text{Top} - \text{Bottom}) / (1 + 10^{((\text{LogEC}_{50} - X) * \text{HillSlope}))}$ , where Y represents the inhibition rate, X is the logarithmic value of the concentration, Top and Bottom are the upper and lower asymptotes of the curve, respectively, HillSlope is the slope of the curve, and LogEC<sub>50</sub> is the logarithmic value of the half-effective concentration. Fitting and calculation were performed using Origin Pro 2025b.

### Statistical analysis

All experiments were conducted with three biological replicates. Data are presented as the mean ± standard deviation ( $\bar{x} \pm s$ ). Data were recorded using Microsoft Excel software. Statistical analysis was performed using SPSS 26.0 software, employing one-way analysis of variance (ANOVA), and t-test and Duncan's test were used for analysis.

### Results

#### Isolation, purification, and screening of actinomycetes

Actinomycetes in the soil samples from healthy *Panax quinquefolius* plants were isolated using GS-1 isolation medium. Strains with consistent colony morphology were merged, and a total of 43 strains were obtained, labeled as XF-1 to XF-43 respectively. Antifungal experiments were conducted to screen the isolated actinomycetes. The results showed that 9 strains exhibited antifungal activity against both test pathogenic fungi, accounting for 20.9% of the total strains. Among these, the inhibition rate of strain XF-3 was significantly higher than that of the other 8 strains ( $p < 0.01$ ): the inhibition rate against *F. solani* was 76.67±1.99%, and the inhibition rate against *F. oxysporum* was 81.6±0.64% (Table 1). Therefore, strain XF-3 was selected for subsequent studies.

**Table-1.** Inhibition effect of 9 strains of actinomycetes on the root rot pathogen of American ginseng.

Strain No	Inhibition rate/%	
	<i>F.solani</i>	<i>F.oxysporum</i>
XF-2	42.00±1.10	32.00±0.20
XF-3	76.67±1.99**	81.67±0.64**
XF-6	33.10±0.15	33.20±0.10
XF-8	44.07±0.80	67.50±0.10
XF-15	32.30±0.95	36.00±0.20
XF-19	50.70±1.39	44.73±0.67
XF-23	58.73±1.01	32.77±1.01
XF-33	50.77±2.34	30.37±0.78
XF-43	50.53±2.26	41.07±0.85

**Note:** Data are presented as mean ± SD. \*\* Indicates extremely significant difference at  $p < 0.01$  (t-test).

### Identification of strain XF-3

#### Morphological identification

Strain XF-3 was capable of growth on all five tested media: ISP3, ISP4, ISP6, CA, and GS-1 (Figure 1). It exhibited the most vigorous growth on ISP6 and GS-1 media, producing abundant aerial mycelia. Growth was moderately robust on ISP3 and ISP4, though

slightly less than on the former two media. On CA medium, the strain showed relatively weak growth, producing sparse or no aerial mycelia, while the substrate mycelia appeared nearly translucent. The cultural characteristics are described in detail in Table 2.



**Figure-1.** Culture characteristics of strain XF-3.

**Table-2.** Culture characteristics of strain XF-3 on different media.

Culture medium	Growth	Substrate hyphae	Aerial hypha	Pigment situation
ISP3	++	white	White、purple gray	yellow
ISP4	++	light yellow	Grey pink、grey white、black brown	light yellow
ISP6	+++	orange-red	dusty pink	orange-red
CA	+	Near transparent color	-	-
GS-1	+++	orange-yellow	white	golden

**Note:** +++: Good growth; ++: Normal growth; +: Poor growth; -: No growth. The same as following.

### Physiological and biochemical identification

Physiological and biochemical experiment results indicate that strain XF-3 can utilize glucose, sucrose, fructose, xylose, etc. as carbon sources, but cannot utilize arabinose as a carbon source; it can utilize glycine, asparagine, arginine, cysteine, histidine, etc. as nitrogen sources, but cannot utilize alanine and aspartic acid as nitrogen sources; it can decompose cellulose, starch, liquefy gelatin, peptize milk, produce urease, but does not produce melanin and H<sub>2</sub>S, and cannot reduce nitrate; it can grow under conditions of

pH>11 and a salt concentration of 6% (Table 3, Table 4). Comparing the identification manual of *Streptomyces* (Yan, 1992) with the above physiological and biochemical results, strains with similar characteristics to it were found to be *S. costaricanus*, *S. murinus* and *S. graminearus*. However, *S. graminearus* does not produce soluble pigments on GS-1 medium, *S. costaricanus* cannot utilize rhamnose and raffinose, and cannot grow in 5% NaCl medium. Based on this comparative analysis, strain XF-3 was preliminarily identified as *S. murinus*.

**Table-3.** Carbon and nitrogen source utilization experiments of strain XF-3.

Carbon source	Growth	Nitrogen source	Growth
glucose	+	glycine	+
rhamnose	+	alanine	-
raffinose	+	aspartate	-
arabinose	-	asparagine	+

**Note:** “+” indicated presence or positive; “-” indicated absence or negative. The same as following.

**Table-4.** Physiological and Biochemical Test Results of Strain XF-3.

Test	Result	Test	Result
Cellulolytic enzyme	+	melanin	-
Amylase	+	H <sub>2</sub> S	-
Urease	+	nitrate reduction	-
pH	2–11	Resistant to NaCl	≤6%

### Molecular identification

The 16S rDNA sequence cloning product of strain XF-3 was sent to Shanghai Sangon Biotech Co., Ltd. for sequencing, yielding a 1422 bp DNA fragment. The sequence was subsequently submitted to the GenBank database and assigned the accession number PV077339. NCBI homology analysis revealed that the 16S rDNA sequence of strain XF-3 showed high

similarity of over 99% with *S. xylanilyticus*, *S. costaricanus*, *S. murinus*, and *S. graminofaciens* strains. In the Neighbor-Joining phylogenetic tree constructed based on 16S rDNA sequences, strain XF-3 clustered together with *S. murinus* (Figure 2). Combined with morphological and physiological-biochemical characteristics, strain XF-3 was finally identified as *S. murinus*.

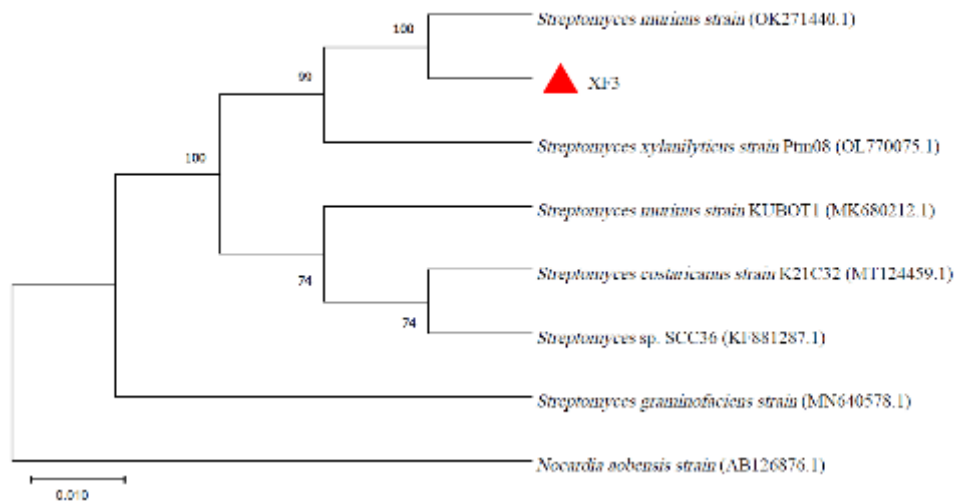


**Figure-2.** Phylogenetic tree of strain XF-3 based on 16S rRNA gene sequence.

### In vitro inoculation of antagonistic bacterial fermentation broth for root control efficacy of ginseng

The control efficacy of strain XF-3 fermentation broth against two pathogenic fungi is shown in Figure 3 and Table 5. American ginseng roots inoculated with *F. oxysporum* (Group 2) exhibited obvious discoloration and rot at the inoculation sites, while roots simultaneously treated with XF-3 fermentation broth (Group 4) showed significantly reduced lesion areas and decreased rotting severity in cross-sections, achieving a relative control efficacy of 66.27%. American ginseng roots inoculated with *F. solani*

(Group 3) developed severe symptoms by day 5, characterized by white mycelium at inoculation sites and soft rot throughout the internal tissues. In contrast, roots co-treated with XF-3 fermentation broth (Group 5) displayed markedly reduced lesion areas and diminished soft rot symptoms in cross-sections, with a relative control efficacy reaching 56.09%. Roots treated only with XF-3 fermentation broth (Group 1) showed slight discoloration at injection sites compared to the sterile water control (CK). These results indicate that strain XF-3 fermentation broth exhibits inhibitory effects against root rot disease in American ginseng caused by both pathogenic fungi.

**Table-5.** Disease prevention effect of fermentation broth of *Streptomyces murinus* XF-3.

Group	Treatment	Disease index	Control effect/%
CK	sterile water	-	-
1	XF-3	-	-
2	<i>F. oxysporum</i>	52.77±4.77 aA	-
3	<i>F. solani</i>	56.93±2.37 aA	-
4	<i>F.oxysporum</i> +XF-3	17.80±2.42 cC	66.27
5	<i>F.solani</i> +XF-3	25.00±0.00 bB	56.09

Note: Data are presented as mean ± standard deviation (SD). Different lowercase letters (a, b, c) indicate significant differences at  $p < 0.05$ , and different uppercase letters (A, B, C) indicate extremely significant differences at  $p < 0.01$  (Duncan's test).

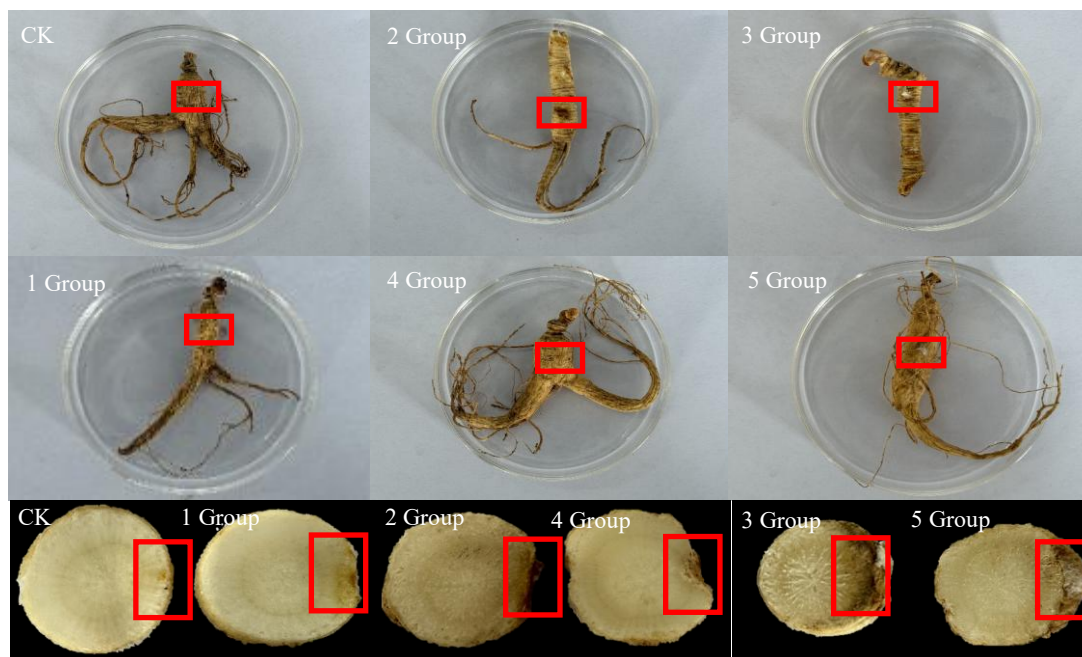


**Figure-3.** Control effect of strain XF-3 fermentation broth on American ginseng.

### Selection results of extractant

By comparing the antifungal activity of active compounds extracted with different organic solvents against *F. oxysporum* and *F. solani*, the results showed that ethyl acetate demonstrated the highest extraction efficiency with inhibition zone diameters of  $37.28 \pm 1.32$  mm and  $36.64 \pm 0.14$  mm, respectively (Table 6). Acetone and n-butanol showed moderate

extraction performance, while petroleum ether exhibited relatively poor extraction efficiency. The inhibition zone diameters for acetone, n-butanol, and petroleum ether were  $29.34 \pm 0.89$  ( $30.01 \pm 0.09$ ) mm,  $29.55 \pm 1.01$  ( $28.96 \pm 0.54$ ) mm, and  $24.01 \pm 1.14$  ( $26.50 \pm 0.13$ ) mm, respectively. Based on the inhibition zone diameter results, ethyl acetate was selected as the optimal solvent for extracting the fermentation broth.

**Table-6.** Extraction effect of different extractants on active substances in XF-3 fermentation broth.

Extractant pathogenic bacteria	Size of antifungal zone/mm			
	Ethyl acetate	Acetone	N-butanol	Petroleum ether
<i>F. solani</i>	$37.28 \pm 1.32$ a	$29.34 \pm 0.89$ b	$29.55 \pm 1.01$ b	$24.01 \pm 1.14$ c
<i>F. oxysporum</i>	$36.64 \pm 0.14$ a	$30.01 \pm 0.09$ b	$28.96 \pm 0.54$ c	$26.50 \pm 0.13$ d

**Note:** Data are presented as mean  $\pm$  SD. Different lowercase letters (a, b, c) indicate significant differences at  $p < 0.05$  (Duncan's test).

### Identification results of active substances in actinomycete strain XF-3

Compound Fr.B is a red powder. Figure 4A shows the  $^1\text{H-NMR}$  spectrum of Fr.B, Figure 4B shows the  $^{13}\text{C-NMR}$  spectrum of Fr.B, and Figure 4C shows the mass spectrum of compound Fr.B. The high-resolution mass spectrum indicates that the mass-to-charge ratio ( $m/z$ )

of compound Fr.B is  $1255.6359$   $[\text{M}+\text{H}]^+$ . The structure of Fr.B was analyzed by  $^1\text{H-NMR}$  and  $^{13}\text{C-NMR}$  spectroscopy. In the  $^1\text{H-NMR}$  spectrum (600 MHz,  $\text{CDCl}_3$ ), signals in the high-field region ( $\delta$  0.75–2.25) correspond to methyl/methylene protons (affected by adjacent hydrogen, unsaturation, or nitrogen effects), while mid-field signals ( $\delta$  2.56–5.94) represent

protons on tertiary carbons (near electron-withdrawing groups) and amino groups. Aromatic/amine protons appear in the low-field region ( $\delta$  7.13–8.21).

In the  $^{13}\text{C}$ -NMR spectrum (151 MHz,  $\text{CDCl}_3$ ), up field signals ( $\delta$  15.1–34.9) correspond to methyl/methylene/tertiary carbons (shifted due to nitrogen or electron-withdrawing groups), aromatic

carbons appear at  $\delta$  101.7–147.5, while downfield signals ( $\delta$  166.3–179.1) correspond to carbonyl groups.

By comparing the mass spectrometry data and nuclear magnetic resonance (NMR) data with known data, the active compound was identified as actinomycin D (Figure 4D).

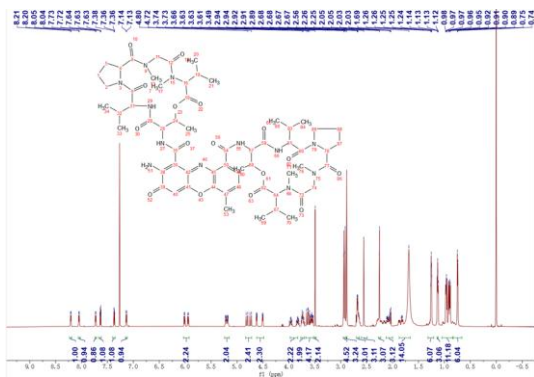


Figure-4A. Fr. B  $^1\text{H}$ -NMR spectrum.

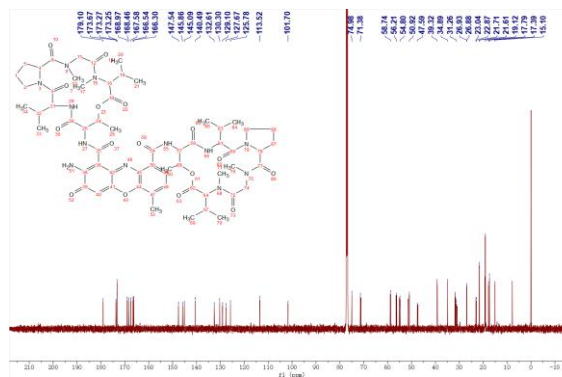


Figure-4B. Fr. B  $^{13}\text{C}$ -NMR

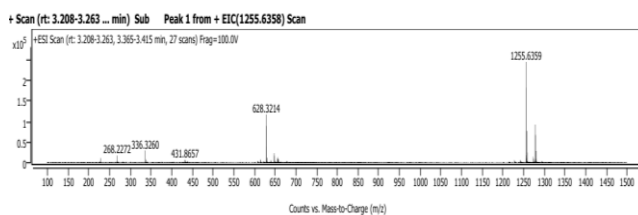


Figure-4C. Mass spectrum of Fr. B

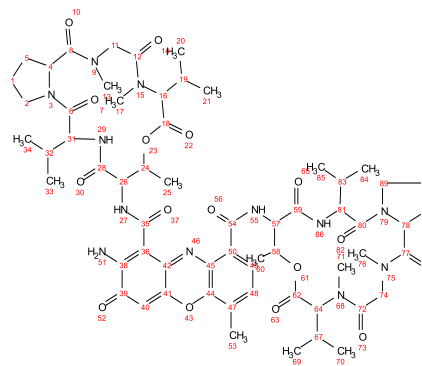
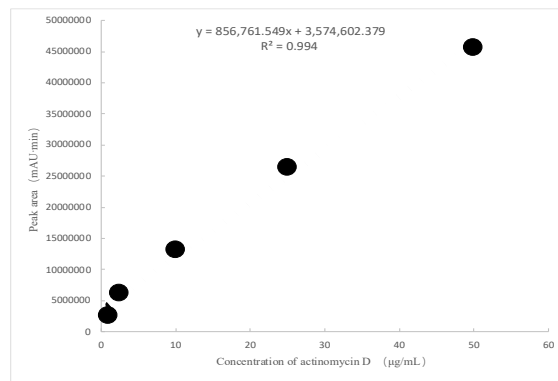


Figure-4D. The structural formula of compound Fr. B.

### Determination results of actinomycin D content in XF-3 fermentation broth

Linear regression analysis was performed on the HPLC peak areas obtained from actinomycin D standard solutions at various concentrations, yielding a linear equation of  $y=850,524.31x+4,025,001.59$  with

a correlation coefficient of  $R^2=0.994$  (Figure 5). By substituting the peak area of the crude extract (diluted 50-fold) into this linear equation, the actinomycin D concentration in the crude extract solution was determined to be  $53.21\pm 1.60$   $\mu\text{g/mL}$ , corresponding to an actinomycin D content of  $44.34\pm 1.33$   $\mu\text{g/mL}$  in the fermentation broth.



**Figure-5.** Standard curve of actinomycin D.

**The effect of actinomycin D on the mycelial growth of *F. oxysporum* and *F. solani***

To determine the inhibitory effects of actinomycin D on mycelial growth of the American ginseng root rot pathogens *F. oxysporum* and *F. solani* (Figure 6C) , mycelial growth diameters were measured under different actinomycin D concentrations, and the EC<sub>50</sub> values were calculated. The results showed that the toxicity regression equation for actinomycin D against *F. oxysporum* was

$$Y = \frac{100}{1 + \left(\frac{X}{11.48}\right)^{-0.78}} \quad (R^2=0.97) \quad (\text{Figure 6B}) ,$$

with an EC<sub>50</sub> value of 11.48 µg/mL (Figure 5). For *F. solani*, the toxicity regression equation was

$$Y = \frac{100}{1 + \left(\frac{X}{2.08}\right)^{-0.82}} \quad (R^2=0.98) \quad (\text{Figure 6A}) ,$$

with an EC<sub>50</sub> value of 2.08 µg/mL. These results indicate that actinomycin D exhibited superior inhibitory effects on mycelial growth of *F. solani* compared to *F. oxysporum*.

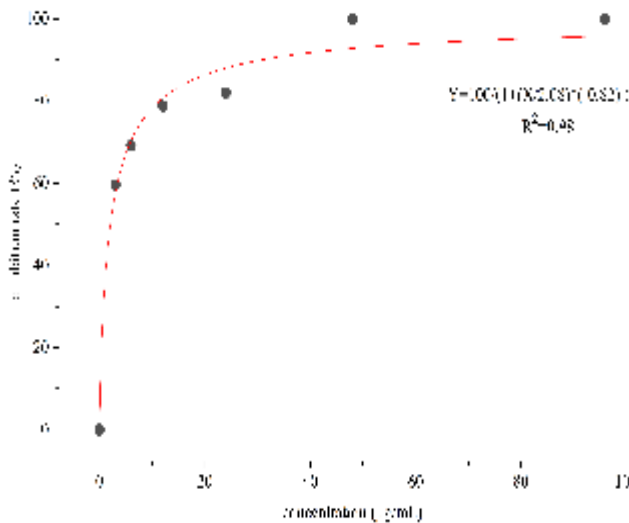


**Figure-6A.** Actinomycin D dose–response curves of *F. solani*

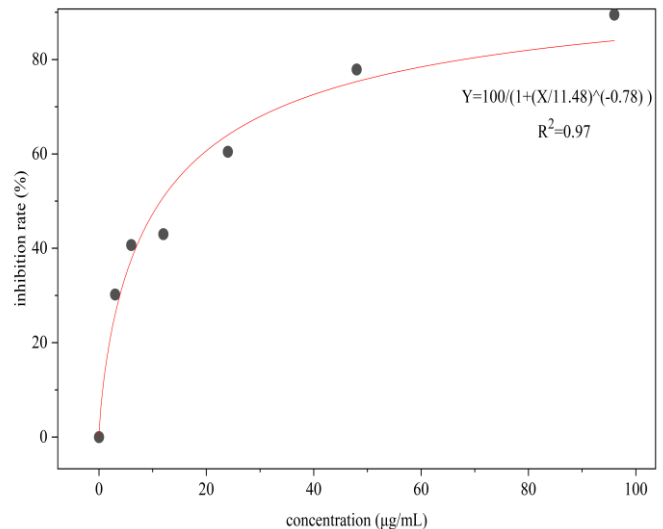
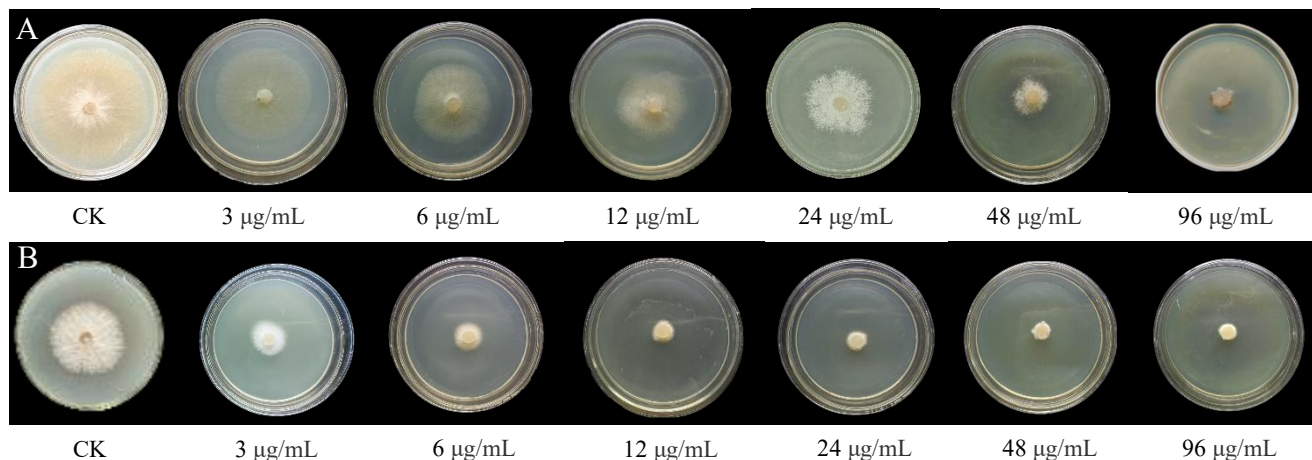


**Figure-6B.** Actinomycin D dose–response curves of *F. oxysporum*



A: The inhibitory effect of different concentrations of actinomycin D on the hyphae of *F. solani* B: The inhibitory effect of different concentrations of actinomycin D on the hyphae of *F. oxysporum*.

**Figure-6C.** The inhibitory effect of different concentrations of actinomycin D on the fungal hyphae of root rot pathogen in American ginseng.

## Discussion

With the increasing public attention to the diseases and safety issues of American ginseng, a large number of studies have been conducted globally to explore novel biological agents. In this study, *S. murinus* XF-3 exhibited significant inhibitory activity against *F. solani* and *F. oxysporum*. Previous studies have shown that *Streptomyces griseus* has good inhibitory effects on eight common plant diseases (Sun, 2024), but there are currently no reports on its effect on the pathogens of American ginseng root rot disease, *F. solani* and *F. oxysporum*. Therefore, it is necessary to conduct a comprehensive study on the antifungal characteristics of this species. This study evaluated the antifungal activity of *S. murinus* against *F. solani* and *F. oxysporum* through in vitro experiments and experiments on infected American ginseng with pathogenic bacteria.

The culture filtrate of *S. murinus* XF-3 exhibited significant inhibitory effects against *F. solani* and *F. oxysporum*, confirming that this strain produces antifungal secondary metabolites—the material basis for biocontrol agents to exert their effects (Ling et al., 2020; Yu et al., 2011). Efficient extraction of target active substances is critical for elucidating biocontrol mechanisms and developing formulations, and solvent selection directly influences extraction efficiency (Zheng et al., 2006). Results showed that ethyl acetate extracts had the highest antifungal activity, while

petroleum ether extracts performed poorest. This discrepancy is closely related to the solubility of actinomycin D: its low solubility in non-polar solvents limits effective enrichment, thereby reducing the overall antifungal activity of the extract, consistent with previous studies on bioactive compound extraction from *Streptomyces* spp. (Yu et al., 2011). The core antifungal metabolite of XF-3 was identified as actinomycin D via column chromatography and NMR spectroscopy. Actinomycin D is a well-documented peptide antibiotic that exerts its effect by binding to the minor groove of DNA, inhibiting RNA synthesis and fungal cell proliferation (Das et al., 2023; Zsiros et al., 2010). While its activity against *Ralstonia solanacearum* and *Magnaporthe oryzae* has been reported, its application has long focused on clinical cancer therapy (Ling et al., 2020). The present study demonstrates strong inhibitory activity against *F. solani* and *F. oxysporum* in vitro, with  $EC_{50}$  values of 2.08  $\mu\text{g/mL}$  and 11.48  $\mu\text{g/mL}$ , respectively. The differential sensitivity between the two pathogens may be attributed to structural differences in their cell walls, *F. solani* has a thinner chitin layer, which facilitates faster penetration of actinomycin D, resulting in higher sensitivity.

The superior biocontrol performance of XF-3 compared to other reported strains such as *S. purpureus* (Zhang et al., 2024) may result from multiple factors. First, XF-3 may possess higher actinomycin D production capacity under

fermentation conditions, leading to greater accumulation of the active compound. Second, actinomycin D produced by XF-3 may exhibit better stability in fermentation broth, maintaining its bioactivity during storage and application. Third, synergistic effects with other co-produced metabolites cannot be excluded, as *Streptomyces* species are known to produce diverse secondary metabolites that may work cooperatively to enhance overall antifungal efficacy. Furthermore, potential interactions between the fermentation broth and host tissue responses may contribute to the observed biocontrol efficacy. The fermentation broth may contain elicitors or signal molecules that induce the host plant's defense responses, such as activation of pathogenesis-related proteins, phytoalexin production, or reinforcement of cell wall structures, thereby enhancing disease resistance through both direct antimicrobial action and indirect immune priming. However, these proposed mechanisms remain speculative and warrant systematic investigation through transcriptomic analysis of treated plants, metabolomic profiling of fermentation broths, and detailed characterization of host-microbe interactions.

However, this study has several limitations that need to be addressed. First, although XF-3 showed promising biocontrol efficacy in detached root assays (56.09% and 66.27% control efficacy against *F. oxysporum* and *F. solani*, respectively), it lacks validation in whole-plant and field trials—environmental factors, soil microbial competition, and XF-3's rhizosphere colonization ability may affect the stability and efficacy of actinomycin D in practical applications (Ji, 2023; Li et al., 2025). Second, actinomycin D's known cytotoxicity raises concerns about potential phytotoxicity to American ginseng and non-target effects on beneficial soil microbes. A comprehensive safety assessment is required before its agricultural application (Huang et al., 1998; Jiao et al., 2019; Chen et al., 2025). Third, the study did not explore the plant growth-promoting potential of XF-3—a trait reported in other biocontrol *S. purpeofuscus* SP3 (Zhu et al., 2013), which exhibits both disease suppression and growth promotion in yew, and this should be a key direction for future research.

Despite these limitations, this study provides valuable baseline data for developing *S. murinus* XF-3 as a biocontrol resource against American ginseng root rot, though substantial work remains before commercial application becomes feasible. Future work will focus on: (1) verifying XF-3's biocontrol efficacy in pot and

field trials; (2) evaluating its growth-promoting effects on American ginseng; (3) optimizing fermentation conditions to enhance actinomycin D production; (4) conducting comprehensive safety assessments including phytotoxicity and environmental impact studies.

## Conclusions

In this study, *Streptomyces murinus* XF-3 isolated from American ginseng rhizosphere soil showed significant antifungal activity against *F. solani* and *F. oxysporum*, with inhibition rates of 76.67% and 81.67%, respectively, and control efficacies of 56.09% and 66.27% in detached root tests. Actinomycin D was identified as the core antifungal metabolite through column chromatography and NMR spectroscopy, with EC<sub>50</sub> values of 2.08 µg/mL and 11.48 µg/mL against the two pathogens, respectively. This study provides new insights into the biocontrol potential of *S. murinus* against American ginseng root rot and expands the agricultural application scope of actinomycin D.

## Acknowledgements

This work was supported by the Shaanxi Key R&D Program (Grant No. 2023-YBNY-091), the Science and Technology Program of Shaanxi Provincial Department of Education (Grant No. 20JS024), the "University-City Co-construction" Scientific Research Special Project of Shaanxi University of Technology (Grant No. SXC-2307), and the Graduate Innovation Fund (Grant No. SLGYCX2526).

**Disclaimer:** None.

**Conflict of Interest:** The authors declare that they have no known competing financial interests or personal relationships that could have appeared to influence the work reported in this paper.

**Source of Funding:** This research was supported by the Key Research and Development Program of Shaanxi Province (Grant No. 2023-YBNY-091); the Science and Technology Program of Shaanxi Provincial Department of Education (Grant No. 20JS024); the "University-City Co-construction" Scientific Research Special Project of Shaanxi University of Technology (Grant No. SXC-2307); and the Graduate Innovation Fund (Grant No. SLGYCX2526).

## Contribution of Authors

YuHao Q & Hao P: Conceptualization of study and designed research methodology.

Hao P: Literature review, data interpretation and funding acquisition.

MeiQi L & WenJing L: Data curation and writing-original draft.

Hong Z & DouDou S: Validation, literature review and editing of the manuscript.

YuSi X: Investigation, data analysis and interpretation

All authors read and approved the final draft of the manuscript.

## References

Cao X, Yang RL and Yuan XW, 2011. Separation, purification, and structural identification of antitumor active components from marine actinomycete ACMA006. *Taiwan Strait*, 30(03): 400–404. DOI: <https://doi.org/10.3969/J.ISSN.1000-8160.2011.03.016>.

Chen DD, Ye JJ, Liang ZY and Xu J, 2025. Preliminary study on the anti-tumor activity mechanism of actinomycin D derived from actinomycetes in mangrove rhizosphere based on a three-dimensional culture model of HepG2 liver cancer cells. *Chin. J. Antibiot.* 8: 902–910. DOI: <https://doi.org/10.13461/j.cnki.cja.007945>.

Das V, Chatterjee NS, Pushpakaran PU, Lalitha KV and Joseph TC, 2023. Exploration of natural product repository by combined genomics and metabolomics profiling of mangrove-derived *Streptomyces murinus* THV12 strain. *Fermentation*. 9(6): 576. DOI: <https://doi.org/10.3390/fermentation9060576>.

Guo RQ, Guan RW and Li HX, 2022. Differential analysis of rhizosphere soil bacterial communities during *Panax quinquefolius* cultivation. *Chin. Arch. Tradit. Chin. Med.* 40(11): 91–94. DOI: <https://doi.org/10.13193/j.issn.1673-7717.2022.11.022>.

Guo YH, Liu SB and Ge QP, 2024. Identification of Actinomycetes 4-1 and study on bacteriostasis and stability of its fermentation broth. *Chin. Agric. Sci. Bull.* 40(09): 117–123. DOI:

<https://doi.org/10.11924/j.issn.1000-6850.casb2023-0135>.

He C and Jia XY, 2009. Identification of autotoxic compounds from fibrous roots of *Panax quinquefolium* L. *Plant Soil*. 318: 63–72. DOI: <https://doi.org/10.1007/s11104-008-9817-8>.

Huang JB, Zhao CS and Zhou MF, 1998. Preliminary study on the biological characteristics of root rot pathogen in American ginseng. *Hubei Agric. Sci.* (05): 33-35. DOI: <https://doi.org/10.3969/j.issn.0439-8114.1998.05.012>.

Huang Q, 2021. Research and development of biocontrol agents for root rot of *Panax quinquefolium*. Ph.D. dissertation, Dali University. DOI: <https://doi.org/10.27811/d.cnki.gdixy.2021.00005>.

Ji L, 2023. Study on soil microbial mechanisms and biocontrol applications in the outbreak of diseases in American ginseng. Ph.D. dissertation, University of Chinese Academy of Sciences. DOI: <https://doi.org/10.27536/d.cnki.gccdy.2023.00018>.

Jiao XL, Zhang XS and Lu XH, 2019. Effects of maize rotation on the physicochemical properties and microbial communities of American ginseng cultivated soil. *Scientific Reports*. 9(1): 8615. DOI: <https://doi.org/10.1038/s41598-019-44530-7>.

Li RJ, Liu JL and Zhang J, 2025. Root rot and control of *Panax quinquefolium*: a review. *Chin. J. Tradit. Chin. Med.* 50(09): 2317–2323. DOI: <https://doi.org/10.19540/j.cnki.cjcmm.20241216.103>.

Li WJ, 2017. Screening and identification of antagonistic actinomycetes of potato fungal diseases. M.S. thesis, Northwest Normal University.

Ling L, Han X and Li X, 2020. A *Streptomyces* sp. NEAU-HV9: isolation, identification, and potential as a biocontrol agent against *Ralstonia solanacearum* of tomato plants. *Microorganisms*. 8(3): 351. DOI: <https://doi.org/10.3390/microorganisms8030351>.

Liu SQ, Zhang JF and Hong MZH, 2025. Isolation and preliminary identification of an antagonistic actinomycetes against *Colletotrichum camelliae*. *Mol. Plant Breed.* 36: 1–20. DOI:

- <https://doi.org/urllid/46.1068.S.20230822.1406.004>.
- National Pharmacopoeia Committee, 2022. *Pharmacopoeia of the People's Republic of China* 2022 Edition, Volume 1. China Medical Science and Technology Press, Beijing.
- National Pharmacopoeia Committee, 2022. *Pharmacopoeia of the People's Republic of China* 2022 Edition, Volume 2. China Med. Sci. Technol. Press, Beijing.
- Sun ZM, Li L and Shen ZZ, 2022. Fermentation condition optimization and stability of *Streptomyces* S-03 strain, a *Phytophthora cinnamomi* antagonist. *Life Sci. Res.* 26(03): 256–263. DOI: <https://doi.org/10.16605/j.cnki.1007-7847.2021.12.0235>.
- Sun ZY, 2024. Research on the *Fusarium graminearum* activity of marine mouse gray *Streptomyces* HN43 and preparation of its biocontrol agents. Ph.D. dissertation, Qufu Normal University.
- Wang Q, Hu Y and Chen S, 2024. Biocontrol efficacy and mechanisms of *Streptomyces purpeofuscus* CC2-6 against Chinese cabbage clubroot caused by *Plasmodiophora brassicae*. *Acta Horticult. Sinica.* 51(05): 1137–1150. DOI: <https://doi.org/10.16420/j.issn.0513-353x.2023-0146>.
- Yan CX, 1992. Classification and identification of actinomycetes. Science Press, Beijing, pp. 268–1048.
- Yan L, Han N and Zhang Y, 2010. Antimycin A18 produced by an endophytic *Streptomyces albidoflavus* isolated from a mangrove plant. *J. Antibiot.* 63(5): 259–261. DOI: <https://doi.org/10.1038/ja.2010.21>.
- Yu L, Dai HF and Wei J, 2011. Bioassay-guided isolation and identification of antibacterial component of *Streptomyces costaricanus*. *Chin. J. Antibiot.* 36(07): 507–510. DOI: <https://doi.org/10.13461/j.cnki.cja.004818>.
- Zhang B, 2014. Isolation, identification and antibacterial activity of endophytic actinobacteria and rhizosphere soil actinobacteria in several medicinal plants. M.S. thesis, Sichuan Agricultural University.
- Zhang JN, Xie TP and Yang LH, 2024. Research progress on root rot disease in medicinal plants. *Chin. Wild Plant Resour.* 43(06): 60–67. DOI: <https://doi.org/10.3969/j.issn.1006-9690.2024.06.009>.
- Zhang MX, Peng N and Wang XX, 2024. Study on the biocontrol effect of antagonistic bacteria XT-25 against *Panax quinquefolium* root rot. *J. Nucl. Agric. Sci.* 38(07): 1249–1257. DOI: <https://doi.org/10.11869/j.issn.1000-8551.2024.07.1249>.
- Zhao FJ, 2020. Preliminary study on the causes and reduction measures of continuous cropping obstacles of *Panax quinquefolium* L. in Liuba, Shaanxi. Ph.D. dissertation, Northwest A&F University. DOI: <https://doi.org/10.27409/d.cnki.gxbnu.2020.01776>.
- Zheng YN, Yang Y and Lü GZ, 2006. Study on the method of actinomycetes isolation from soil. *Anhui Agric. Sci.* 34(06): 1167–1168+1170. DOI: <https://doi.org/10.13989/j.cnki.0517-6611.2006.06.070>.
- Zhu TH, Zhang LN, Li SJ, et al., 2013. Strain of *Streptomyces purpurea* SP3 and its application in yew soil-borne root disease and growth promotion of yew: CN201210367119.3. 2013-12-18.
- Zsíros J, Maibach R, Shafford E, Brugières L, Brock P, Roebuck D and Perilongo G, 2010. Successful treatment of childhood high-risk hepatoblastoma with dose-intensive multiagent chemotherapy and surgery: final results of the SIOPEL-3HR Study. *J. Clin. Oncol.* 28(15): 2584–2590. DOI: <https://doi.org/10.1200/JCO.2009.22.4857>.